Photochemical & Photobiological Sciences

PAPER

Cite this: *Photochem. Photobiol. Sci.*, 2016, **15**, 879

Biospectroscopy, biospectrometry and imaging of *Ilex paraguariensis*. Basis for non-destructive quality evaluation using artificial vision†

Tamara L. Parapugna,[a] Gabriela Petroselli,[b] Rosa Erra-Basells[b] and M. Gabriela Lagorio*[a]

Received 24th February 2016,
Accepted 25th May 2016

DOI: 10.1039/c6pp00054a

www.rsc.org/pps

Yerba mate (YM) is massively produced and consumed as an infusion in South America and is gaining popularity all over the world. This product is obtained from the dried leaves of *Ilex paraguariensis* Saint Hilaire, mixed with fragments of its dried branches. For its commercialization YM must have a minimum percentage of leaves according to a standard classification. Until now, composition quantification has been mechanically performed, thus development of new methods is still pending. In this work a quantification method using solid-phase molecular fluorescence, alternately diffuse reflectance spectroscopy and an imaging technique using a scanner have been proposed. Strong differences between the spectroscopic properties of leaves and sticks were observed and in all the cases linear correlations between the processed signals and composition were observed. Interesting differences in chemical composition of YM leaves and sticks were additionally obtained in this work by means of total phenol content quantification, ultraviolet matrix assisted laser-desorption ionization mass spectrometry and ultraviolet laser-desorption ionization mass spectrometry.

Introduction

Water infusions from dry leaves and sticks of *Ilex paraguariensis* have been prepared and consumed by the people of South America since precolumbian times.[1] These herbal teas are rich in polyphenols and have beneficial health properties as antifungal, antioxidant, anti-inflammatory, anticancer and antiatherosclerosis agents.[1–5] Correlations between the total polyphenolic content of yerba mate infusions and their antioxidant activity have been presented in the literature.[6]

Ilex paraguariensis is marketed as Yerba Mate (YM) consisting in a mixture of dried leaves, slightly toasted and milled, generally mixed with fragments of young dried branches, petioles and peduncles. The percentage of leaves and sticks (broken or powdered) determines the YM quality. The content of leaves, as required by the Argentine food code for the commercial product,[7] should be greater than a given set value (65% for YM with sticks and 90% for YM without sticks). This code establishes a mechanical methodology through the use of different sieves to determine the relative amount of sticks and leaves.[7] In this context, it would be attractive to find optical fingerprints for leaves and for sticks that allow one to develop a fast methodology for estimating the composition of YM. The analysis of the interaction between light and biological matter (biophotonics) is relevant in the development of light-based devices that will serve as tools for non-destructive monitoring and quality assessment.[8] Particularly for food, vegetables, herbs and spices, these methods may not only provide information on quality but also on the nutraceutical content.[9,10]

Several chromatography and mass spectrometry techniques have been previously used to study the composition of YM. For instance, a liquid chromatography (LC) method was developed and validated for identification and quantification of polyphenols in aqueous solution from yerba mate by Amaral da Silva *et al.*[11] UPLC-PDA-MS analysis of YM compounds including new saponins was performed by de Souza *et al.*[12] Polycyclic aromatic hydrocarbon (PAH) contents in YM infusions were determined by high performance liquid chromatography using fluorescence detection (HPLC-FLD) by Thea.[13] A two-dimensional liquid chromatography (LC × LC) system with a diode array (DAD) and electrospray/ion trap-time of flight (ESI/IT-TOF) as detection allowed unequivocal identification of

[a]*INQUIMAE-CONICET/Dpto. de Química Inorgánica, Analítica y Química Física, Facultad de Ciencias Exactas y Naturales, Universidad de Buenos Aires, Pabellón II, 1er piso, C1428EHA, Buenos Aires, Argentina. E-mail: mgl@qi.fcen.uba.ar; Fax: +5411 4576 3341; Tel: +5411 4576 3378 ext. 106*

[b]*CIHIDECAR-CONICET/Dpto. de Química Orgánica, Facultad de Ciencias Exactas y Naturales, Universidad de Buenos Aires, Pabellón II, 3er piso, C1428EHA, Buenos Aires, Argentina*

†Electronic supplementary information (ESI) available: Fig. S1–S9. See DOI: 10.1039/c6pp00054a

several compounds (caffeine, theobromine, theophylline, gallic acid, chlorogenic acid, catechin, caffeic acid, rutin and quercetin) in the mate extracts according to Dugo *et al.*[14] Chlorogenic acid (CGA) composition of some plants including yerba mate was determined by HPLC-UV and LC-DAD-ESI-MS by Marques *et al.*[15]

In another study, the phenolic profiles in organic extracts from YM were characterized by direct infusion electrospray insertion mass spectrometry (ESI-MS) by Markowicz Bastos.[16] Phenolics, xanthines, and carbohydrates were identified and quantified by electrospray ionisation mass spectrometry (ESI-MS) and ultra performance liquid chromatography (UPLC), in the samples of aqueous extraction from YM leaves by Dartora *et al.*[17] HPLC-DAD-ESI/MS was used for the identification and quantification of caffeoylquinic acids (CQA), flavonol glycosides and purine alkaloids in mate infusions by Peres *et al.*[18] Major volatile compounds were identified by GC-MS; among them, norisoprenoid compounds were identified by Márquez.[19]

In previous studies reported by other authors, infusions of yerba mate prepared as traditionally consumed in South America (hot mate or just mate, and cold mate or tereré)[12] or organic extracts of mate have been analyzed.[13]

According to a recent survey of the literature, to date no research has been reported using ultraviolet matrix assisted laser desorption-ionization mass spectrometry (UV-MALDI-MS) and/or ultraviolet laser desorption–ionization mass spectrometry (UV-LDI-MS) for the study of YM samples (neither individual parts of the plant nor infusions). However, in a recent publication phenolic compounds present in methanolic/water extracts from stems and from leaves have been analyzed by ESI-MS.[20]

In the present work we have studied in detail the spectroscopic and optical behaviour of YM sticks, YM leaves and their mixtures in order to set base for the development of non-destructive methods to perform quality assessment. In this way, the main purpose of this work was the search for new and fast optical methodologies as alternatives to slow standard methods of YM analysis. Additionally, the UV-MALDI-MS and the UV-LDI-MS techniques were used on this material for the first time, to identify distinctive chemical composition profiles for YM leaves and sticks.

Experimental

Samples

Experiments were performed on samples of *Yerba Mate Elaborada con Palo* (Yerba Mate with Stems) from a commercial brand. Leaves and sticks were manually separated with a tweezer and respectively pulverized in a mortar. Mixtures with different composition of leaves and sticks were prepared.

Solid-phase molecular fluorescence

Fluorescence spectra of the samples were obtained using a steady-state spectrofluorometer (QuantaMaster, PTI – Photon Technology International – Brunswick) in the front phase geometry. A 75 W Xenon lamp was used as the excitation source and the incidence and detection angles were set to 30° and 60°, respectively. The excitation wavelength ranged from 300 to 400 nm. The emission wavelength ranged from 320 to 800 nm correspondingly and spectra were corrected for the detector response to different wavelengths.

Spectra were recorded for layers of mixtures of YM components.

Diffuse reflectance spectroscopy

Diffuse reflectance was recorded as a function of wavelength from 350–800 nm for different optically thick samples (2 mm) of YM leaves, YM sticks and their mixtures. A spectrophotometer (UV3101PC, Shimadzu, Tokyo, Japan) equipped with an integrating sphere (ISR-3100, Shimadzu, Tokyo, Japan) was used for the measurements. Barium sulfate was used as 100% reflectance (white reference). From the reflectance data, the remission function, a quantity proportional to the chromophore concentration in the sample was also calculated as $F(S) = [1 - S(\lambda)]^2/[2S(\lambda)]$.[21,22] From reflectance spectra colour coordinates were additionally calculated for each sample.

Colour coordinates from reflectance

From the reflectance spectrum defined as $S(\lambda)$ of the samples, it was possible to calculate the tristimulus values X, Y, Z using eqn (1)–(4).[23]

$$X = \frac{1}{N}\int_{\lambda} \bar{x}(\lambda)S(\lambda)I(\lambda)\mathrm{d}\lambda \quad (1)$$

$$Y = \frac{1}{N}\int_{\lambda} \bar{y}(\lambda)S(\lambda)I(\lambda)\mathrm{d}\lambda \quad (2)$$

$$Z = \frac{1}{N}\int_{\lambda} \bar{z}(\lambda)S(\lambda)I(\lambda)\mathrm{d}\lambda \quad (3)$$

$$N = \int_{\lambda} \bar{y}(\lambda)I(\lambda)\mathrm{d}\lambda \quad (4)$$

In these equations $\bar{x}$, $\bar{y}$ and $\bar{z}$ are the functions defined by the CIE 1931 standard observer and $I(\lambda)$ is the spectral distribution of a reference illuminant (D65 in this case). N is a normalization factor. The $\bar{y}$ colour function matches the spectral response of the human eye. Differently, $\bar{x}$ and $\bar{z}$ do not correspond directly to a real phenomenon. By convention, the normalization factor is defined by eqn (4), so that the tristimulus value Y equals unity when the reflectance is 1 for all wavelengths. It should be noted that using this convention, the colour coordinate Y of the source light is also set to unity. The integrals were computed over the visible-NIR spectrum (360–830 nm). In this work, the colour space sRGB was used. From colour coordinates X, Y, and Z in the nominal range (0–1), RGB values were obtained according eqn (5)–(9).

$$\begin{bmatrix} r \\ g \\ b \end{bmatrix} = [\mathrm{M}]^{-1} \begin{bmatrix} X \\ Y \\ Z \end{bmatrix} \quad (5)$$

where

$$[\mathrm{M}]^{-1} = \begin{bmatrix} 3.2406 & -1.5372 & -0.4986 \\ -0.9689 & 1.8758 & 0.0415 \\ 0.0557 & -0.2040 & 1.0570 \end{bmatrix} \quad (6)$$

$$R = \begin{cases} 12.92\, r & r \leq 0.0031308 \\ 1.055\, r^{\frac{1.0}{2.4}} - 0.055 & r > 0.0031308 \end{cases} \quad (7)$$

$$G = \begin{cases} 12.92\, g & g \leq 0.0031308 \\ 1.055\, g^{\frac{1.0}{2.4}} - 0.055 & g > 0.0031308 \end{cases} \quad (8)$$

$$B = \begin{cases} 12.92\, b & b \leq 0.0031308 \\ 1.055\, b^{\frac{1.0}{2.4}} - 0.055 & b > 0.0031308 \end{cases} \quad (9)$$

Finally to express R, G and B values in the range (0255) each component was multiplied by 255.[23]

Imaging

Scans were recorded for layers of mixtures of YM components using an Epson Stylus Office TX300F scanner. Images were processed with the Adobe Photoshop CC software program. From selections of 80 880 pixels, medium values of R, G, B with their respective standard deviations were obtained.

Total polyphenol concentration (TPC)

A modification of the Folin–Ciocalteu method previously described[24] was used for the measurement of the total content of phenolic compounds. Briefly, herbal teas were prepared from aqueous suspensions (1.00% m/m) boiled for 10 minutes at 98 °C. The mixtures were cooled to room temperature before filtration with Whatman no. 4 filter paper and the volume made up to maintain the initial concentration. The extracts were suitably diluted and immediately used for TPC determination. One milliliter of the diluted extracts was mixed with 1.0 ml of the Folin reagent (Folin–Ciocalteu's phenol reagent, Sigma Aldrich). This mixture was allowed to stand for 2–5 min before the addition of 2 ml of 20% Na_2CO_3. After a 10 minute incubation at room temperature the absorbance was measured at 730 nm on a Shimadzu 3100 Spectrophotometer. The standard curve was prepared with known concentrations of gallic acid (Sigma Aldrich).

UV-MALDI-MS and UV-LDI-MS analysis

Ultraviolet matrix assisted laser desorption–ionization mass spectrometry (UV-MALDI-MS) and ultraviolet laser desorption-ionization mass spectrometry (UV-LDI-MS) were performed on the Bruker Ultraflex Daltonics TOF/TOF mass spectrometer. Mass spectra were acquired in linear positive and negative ion modes and with the LIFT device in the MS/MS mode. The solid samples (leaves and sticks smashed in a mortar) were suspended in water and transferred to the electrode (probe) as soon as possible. Measurements were also performed on infusions from sticks and leaves prepared as described above for TPC. The effect of the addition of TFA or NaCl to the samples was also studied. External mass calibration was performed

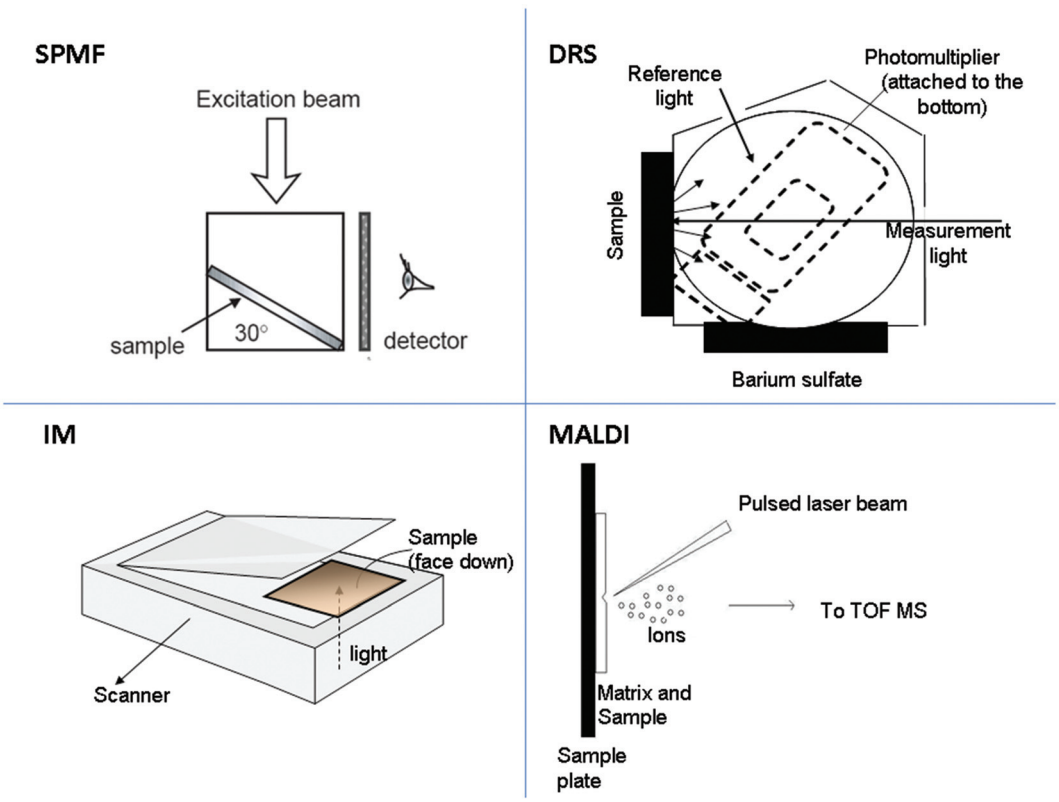

Scheme 1 Schematic diagrams illustrating measurement geometries used in SPMF, DRS, IM and MALDI.

using β-cyclodextrin (MW 1134) with 9*H*-pyrido[3,4*b*]-indole (norharmane, nHo) as a matrix in positive and negative ion mode. The matrix signal was used as an additional standard for calibration in both ion modes. The sample solutions were spotted on a MTP 384 target plate polished steel from Bruker Daltonics (Leipzig, Germany). For UV-MALDI-MS matrix solutions were prepared by nHo (1 mg ml^{-1}), 2,5-dihydroxybenzoic acid (gentisic acid, GA; 3 mg ml^{-1}), 3,4-dimethoxy-4-hydroxycinnamic acid (sinapinic acid, SA; 2 mg ml^{-1}) in acetonitrile/water (1 : 1, v/v). For UV-MALDI-MS experiments a sandwich method was used according to Nonami *et al.*[25] loading successively 0.5 μl of the matrix solution, analyte solution and matrix solution after drying each layer at normal atmosphere and room temperature. The matrix to analyte ratio was 3 : 1 (v/v) and the matrix and analyte solution loading sequence was: (i) matrix, (ii) analyte, (iii) matrix, (iv) matrix. For UV-LDI-MS experiments two portions of the analyte solution (0.5 μl × 2) were loaded on the probe and dried successively (two dry layers). Desorption/ionization was obtained by using a frequency-tripled Nd:YAG laser (355 nm). Experiments were performed using firstly the full range setting for laser firing position in order to select the optimal position for data collection, and secondly fixing the laser firing position in the sample sweet spots. The laser power was adjusted to obtain a high signal-to-noise ratio (S/N) while ensuring minimal fragmentation of the parent ions and each mass spectrum was generated by averaging 100 laser pulses per spot. Spectra were obtained and analyzed with the programs FlexControl and FlexAnalysis, respectively. nHo, GA, SA and β-cyclodextrin (cyclomaltoheptaose) were purchased from Sigma-Aldrich Chemical Co. Trifluoroacetic acid was purchased from Merck. Water of very low conductivity (Milli Q grade) was used.

Schematic diagrams illustrating measurement geometries used in each method are shown in Scheme 1.

Results and discussion

Solid-phase molecular fluorescence

The UV-light induced fluorescence spectra from the YM samples have essentially shown two types of emissions: one in the blue-green and the other in the red-far-red portion of the spectra (Fig. 1). The blue fluorescence emission (BF, λ_{max} near 450 nm) from plants is due to phenolic substances such as chlorogenic, caffeic, ferulic, rosmarinic and coumaric acids.[26,27] Quercetin was reported to contribute to green fluorescence (GF, λ_{max} near 530 nm) broadening the BF peak[28] but some authors questioned if this contribution is actually relevant.[10] Caffeic acid, chlorogenic acid and quercetin have been already reported to be present in mate tea[1] and they are most likely to be responsible for the blue-green fluorescence observed in this work. Chlorophyll-*a* is responsible for the observed red (RF, 680 nm) and far-red (FRF, 716 nm) fluorescence.[29–31] Excitation of YM from 300 to 400 nm leads to fluorescence emission peaking in the blue-green and in the red-far-red portion of the spectra. Fluorescence ratios of

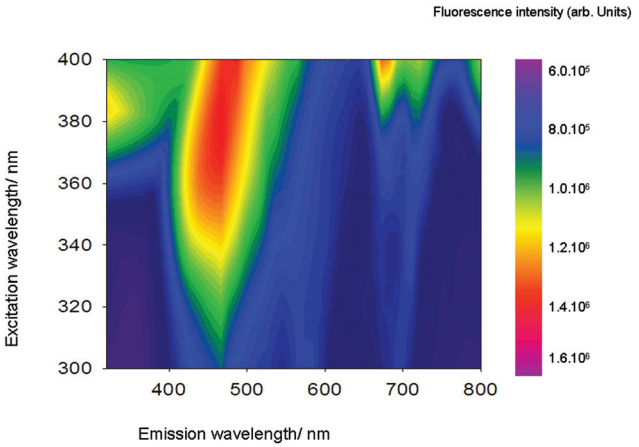

Fig. 1 Fluorescence excitation-emission matrix of YM.

intensities at maxima for shorter to longer wavelengths were calculated for each excitation wavelength. Results for 100% sticks and 100% leaves are shown in Fig. 2.

The fact that ratios BF/RF differed between sticks and leaves, motivated the extension of this analysis for several compositions of both the constituents. A value of 360 nm was selected for the excitation wavelength as it leads to a higher difference between the signals for sticks and leaves.

Emission spectra (λ_{exc} 360 nm) for a set of samples are shown in Fig. 3. The processed signal ($BF_{469\ nm}/RF_{680\ nm}$ ratios) correlated linearly with composition as it may be seen in Fig. 4. Analogous correlations were found for other excitation wavelengths (results not shown).

This linear correlation between the fluorescence ratio and the proportion of sticks may be interpreted in terms of an averaged input from the fluorescence of leaves and sticks. In fact, for a fixed excitation wavelength, considering independently the emission of fluorescent compounds in leaves and sticks, the ratio blue/red for the sample may be considered as the

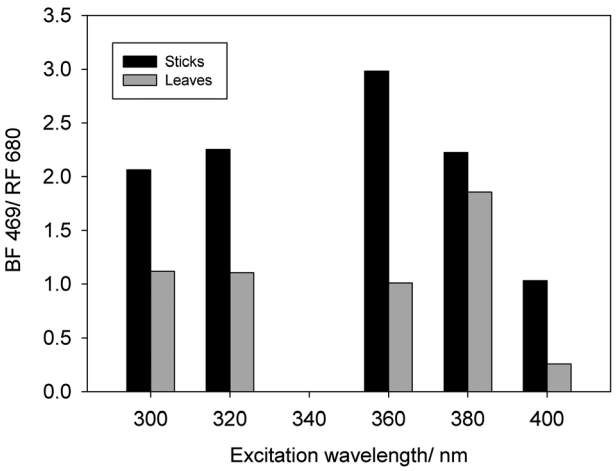

Fig. 2 Blue to red fluorescence ratio (BF 469/RF 680) for sticks and for leaves separately, after excitation with different wavelengths.

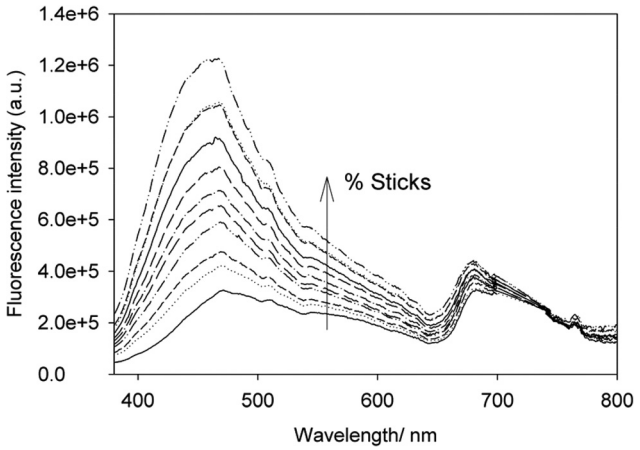

Fig. 3 Fluorescence emission spectra of YM samples with different stick contents. Excitation wavelength: 360 nm.

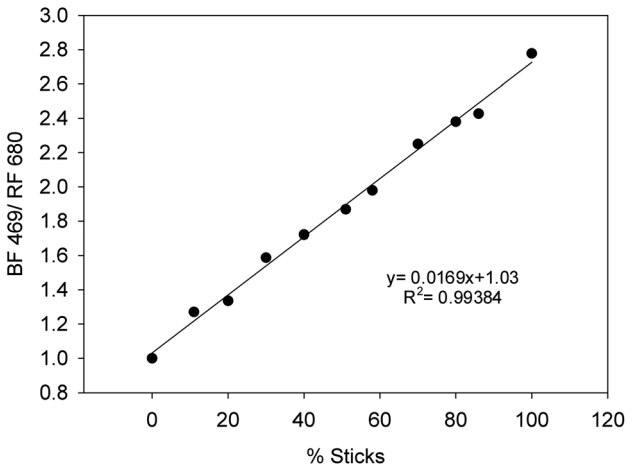

Fig. 4 Blue to red fluorescence ratio (BF 469/RF 680) as a function of stick content (mass percentage) in YM samples. Excitation wavelength: 360 nm. Standard errors for the linear fit: ±0.0004 (slope), ±0.02 (intercept).

weighted average of the contribution of leaves and sticks (eqn (10)):

$$\frac{m_L}{m_T}\left(\frac{BF}{RF}\right)_L + \frac{m_S}{m_T}\left(\frac{BF}{RF}\right)_S = \left(\frac{BF}{RF}\right)_T \quad (10)$$

where m represents the mass and the subscripts L, S and T stand for leaves, sticks, and total YM respectively.

Taking into account that the total mass of the sample is the sum of the masses of leaves and sticks:

$$m_L + m_S = m_T \quad (11)$$

Eqn (12) is easily deduced from eqn (10):

$$\left(\frac{BF}{RF}\right)_L + \frac{m_S}{m_T}\left[\left(\frac{BF}{RF}\right)_S - \left(\frac{BF}{RF}\right)_L\right] = \left(\frac{BF}{RF}\right)_T \quad (12)$$

The applicability and goodness of this approach to our set of data was validated not only by the linear correlation obtained (Fig. 4) but also by comparing the line intercept with the averaged experimental values (BF/RF) for leaves and the slope of the graph with the difference for BF/RF between sticks and leaves. The agreement between the compared values was very good (relative difference less than 14%).

Diffuse reflectance spectroscopy

Reflectance of the samples increased as the proportion of sticks was augmented (Fig. 5). Actually, a linear correlation between reflectance and YM composition was obtained (Fig. 6). Thus, it was proved experimentally here that the reflectance measured for the whole sample could be interpreted as a linear combination of the reflectance of separate sticks and leaves. From a theoretical point of view, this kind of behaviour is present whenever particles are much larger than the wavelength of the excitation light and the spatial scale of the mixture is higher than the average photon path length.[32–34] The remission function which is usually connected directly

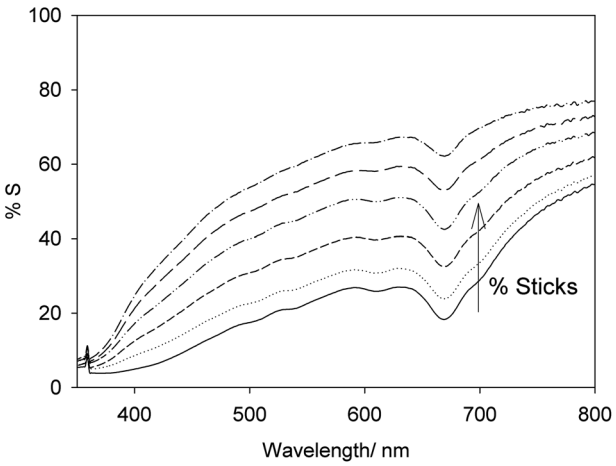

Fig. 5 Reflectance spectra of YM with different contents of sticks.

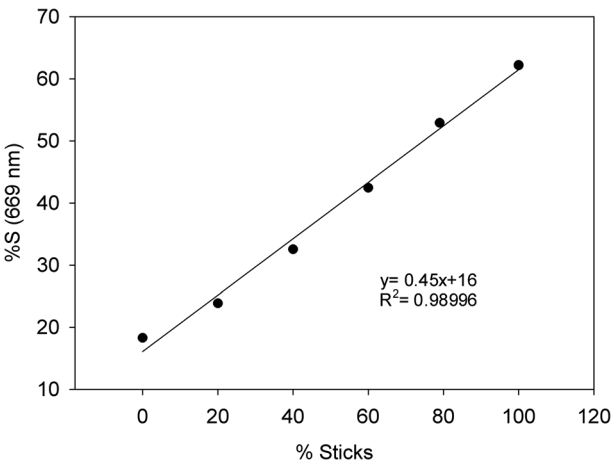

Fig. 6 Percent reflectance at 669 nm as a function of stick content (mass percentage) in YM samples. Standard errors for the linear fit: ±0.02 (slope), ±1 (intercept).

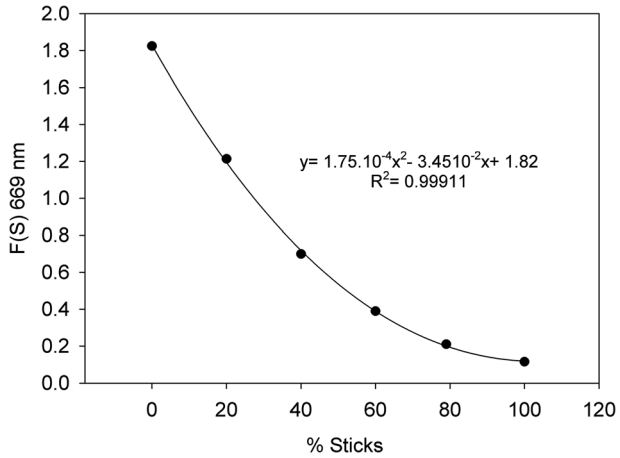

Fig. 7 Remission function as a function of stick content (mass percentage) in YM samples. Standard errors for the polynomial fit: $\pm 8 \times 10^{-6}$ (a_2), $\pm 8 \times 10^{-4}$ (a_1), $\pm 2 \times 10^{-2}$ (a_0).

with the chromophore concentration did not show a linear dependency when plotted *vs.* sticks percentage, but fitted to a quadratic function instead (Fig. 7).

Colour coordinates from reflectance

Colour coordinates (*R*, *G* and *B*) obtained from reflectance spectra were plotted as a function of stick content. Values for each colour component increased linearly as the percentage of sticks increased (Fig. 8). Linear mixing of signals with very good correlation coefficients (particularly for the red component) was also observed in this case.

Image technique

Colour coordinates (*R*, *G* and *B*) obtained from scanned images of the samples with different compositions were

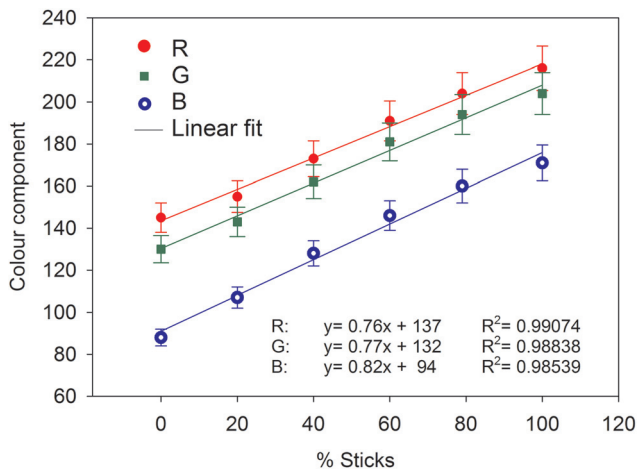

Fig. 8 Correlations between the stick content (mass percentage) and the values of the coordinates *R*, *G*, and *B* obtained from reflectance spectra. Standard errors for the linear fits: *R*: ±0.03 (slope), ±2 (intercept), *G*: ±0.03 (slope), ±2 (intercept), *B*: ±0.04 (slope), ±3 (intercept).

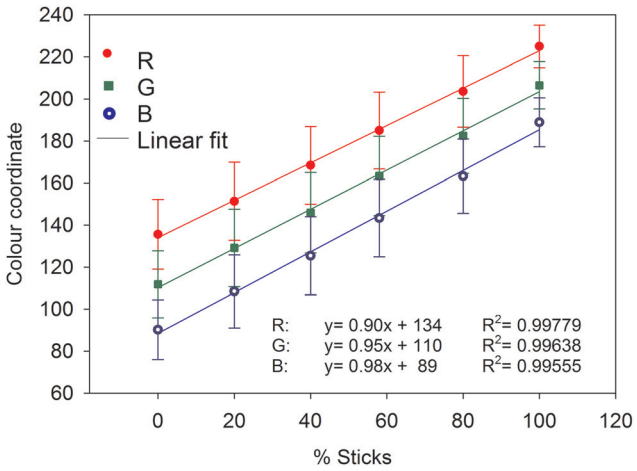

Fig. 9 Correlations between the stick content (mass percentage) and the values of the coordinates *R*, *G*, and *B* obtained from scanned images. Standard errors for the linear fits: *R*: ±0.02 (slope), ±1 (intercept), *G*: ±0.03 (slope), ±2 (intercept), *B*: ±0.02 (slope), ±2 (intercept).

plotted as a function of stick content (Fig. 9). Excellent linear correlations were obtained.

Total polyphenol concentration (TPC)

In order to obtain information on the phytochemical composition of the YM samples, total polyphenol concentration was determined in water infusions. YM tea like infusion is not strictly the usual way of consumption by people in south America as they mainly prepare a beverage by repeatedly pouring very hot water over the YM until it loses its flavor. However, differences between sticks and leaves are best compared using YM infusions (Fig. 10). The obtained concentration of polyphenols in the samples ranged from 29.5 ± 0.5 (for the sample containing 0% leaves) to 110.0 ± 0.5 (for the sample containing 100% leaves) mg equiv. gallic acid per g of

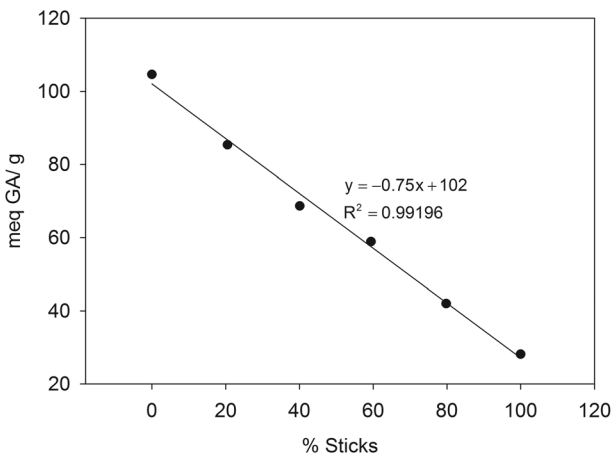

Fig. 10 Correlation between the polyphenolic content of YM infusions, determined by the Folin–Ciocalteu method, and the stick content (mass percentage). Standard errors for the linear fit: ±0.03 (slope), ±2 (intercept).

the dry sample. These results are in agreement with previously published values of 77.6 ± 2.7 to 81.2 ± 4.0 mg equiv. gallic acid per g dry sample[6] and 94.91 ± 4.18 mg equiv. gallic acid per g dry YM tea for commercial brands.[35] Our results confirm that the TPC for leaves is higher than for sticks. As a consequence, the mixture of sticks with YM dry leaves leads to a decrease in its quality from a nutraceutical point of view. YM is an important source of polyphenols, comparable to tea and orange juice.[6,36] Previously, da Silva *et al.* have stated that YM, in addition to its stimulant and nutritional properties, is an important source of antioxidants.[37] In fact, our results showed that drinking 0.5 L of infusion (usually prepared with 50 g of dry YM) provides an intake of about 0.5 g of polyphenols.

UV-MALDI-MS and UV-LDI-MS analysis

Yerba mate samples studied in this work showed strong absorption in the UV–vis region, particularly at 355 nm (Fig. 5). This property allowed to desorb and ionize them using a UV laser without needing the presence of a secondary molecule as a photosensitizer or a matrix in the sample (UV-laser desorption ionization mass spectrometry, UV-LDI-MS). However, for comparison purposes, we also recorded the mass spectra, adding a MALDI matrix in the sample (UV-MALDI-MS). For the latter experiments, nHo, GA and SA were chosen as matrixes.

Fig. S1a (Fig. S1–S9 are included in the ESI†) shows negative ion UV-LDI mass spectrum of the leaf samples after being smashed in a mortar. It was possible to detect and identify some compounds: GA at m/z = 153.038, quinic acid at m/z = 191.191, chlorogenic acid at m/z = 353.68, and rutin at m/z = 609.873. The laser power was adjusted to obtain a high signal-to-noise ratio (S/N) while ensuring minimal fragmentation of the parent ions. However, some fragmentation was observed. For instance, the loss of the disaccharide rutinose moiety from the rutin yields a signal at m/z = 301.528 (flavonol quercetin moiety). The spectrum was recorded also for stick samples after they were smashed in a mortar (Fig. S1b†). A lower number of compounds were detected in that spectrum compared with the one obtained from leaves. Only GA at m/z = 153.020, quinic acid at m/z = 191.201 and chlorogenic acid at m/z = 353.715 were identified. No significant differences were observed in UV-LDI mass spectra when a hot water infusion from leaves was used instead of the sample smashed in a mortar (results not shown). Similar results were obtained for sticks (results not shown).

UV-MALDI mass spectra for water infusions were recorded in negative mode using nHo as a MALDI matrix. As shown in Fig. S2a† and in comparison with the UV-LDI-MS spectrum obtained for the leaf samples, two additional compounds, were detected at m/z = 515.174 and m/z = 677.402 corresponding to dicaffeoylquinic and tricaffeoylquinic acid, respectively. On the other hand, rutin and tricaffeoylquinic acid were not detected in the stick samples (Fig. S2b†). No significant differences in the spectra were observed when different sizes of particles (smashed samples) were studied (data not shown).

UV-MALDI MS/MS spectra of precursor ions at m/z = 514.007 and at m/z = 608.991 were recorded in order to characterize the compounds as dicaffeoylquinic acid and rutin respectively (Fig. S3 and S4†). The successive loss of two caffeoyl moieties from the former was observed (Fig. S3;† fragments at m/z 352.082 and 190 218, $\Delta m/z$ 162); taking into account the intensity ratio of ions at m/z 515 and 353 here observed and the fragmentation pattern previously described in the literature, for dicaffeoylquinic isomeric acids,[17] the structure corresponding to 3,4-dicaffeoylquinic acid can be inferred. Rutin showed the expected fragment at m/z 299.754 (Fig. S4†) as it has been described in the literature.

Additional information was obtained from spectra recorded in negative and positive ion modes. For the leaf samples, signals at m/z 1057, 1073 and 1219 in negative ion mode and the corresponding $[M + Na]^+$ species in positive ion mode at m/z 1082, 1098 and 1244 (Fig. S5a and S5b†) were observed. For the stick samples, only one of these signals was detected at m/z 1073 (negative ion mode) and the corresponding $[M + Na]^+$ ion at m/z 1098 (positive ion mode) (Fig. S6†). Similar results were obtained for smashed and hot water infusion from leaves and sticks. Spectra obtained in negative ion mode showed quite broad low intensity signals while higher resolution spectra with a better signal to noise ratio were obtained in positive ion mode. Saponins, named matesaponins, have been reported in YM.[17,38] As it has been confirmed, UV-MALDI MS/MS analysis (positive ion mode) for precursor ions at m/z 1082.037, 1098.451 and 1244.079 (Fig, S7a, S8 and S7b,† respectively) the matesaponin 2, matesaponin 3 and matesaponin 4, fully characterized by Gosman and Guillaume,[38] are present in the samples from leaves. For the stick samples, the MS/MS spectrum obtained from a precursor ion at m/z 1098.284 (Fig. S9†), in the same ion mode, showed a different fragmentation pattern from that observed for the precursor ion at m/z 1098.452 from the leaf samples (Fig. S8†). Thus the presence of a matesaponin 3 like isobaric compound in sticks can be inferred from the present results.

Besides, disaccharides and trisaccharides were detected in positive ion mode; the former at m/z = 365 and m/z = 381 as sodium and potassium adducts, respectively, and the latter at m/z = 527 and m/z = 543 as sodium and potassium adducts too (results not shown).

An outstanding chemical aspect arising from MALDI analysis is that the polyphenolic flavonoid rutin, the 3,4-dicaffeoylquinic acid (a hydroxycinnamic acid) and matesaponins 2 and 4 are present in leaves and absent in sticks (both smashed samples and hot water infusion). Both of them present significant healing properties. Rutin was reported to have relevant nutraceutical properties in: anti cancer activity,[39] protection of blood vessels,[40] prevention of cardiovascular diseases,[41] anti-hyperglycaemic and antioxidant activity in diabetic rats,[42] the improvement of spatial memory in Alzheimer's disease due to anti-oxidant and anti-inflammatory activity,[43] arthritis treatment as an anti-inflammatory drug,[44] and antifungal activity[45] among others.

Furthermore, dicaffeoylquinic acids (ester formed from quinic acid and two units of caffeic acid) were reported to have antioxidant properties through direct scavenging on free radicals.[45,46] The isomer 3,5-dicaffeoylquinic acid was proved to be an antioxidant and anti-inflammatory drug[47] and several isomers (3,4; 4,5 and 1,5) of dicaffeoylquinic acid displayed antiviral activity against HIV.[48] Several isomers of dicaffeoylquinic acid also presented a hepatoprotective effect in previously published studies.[49,50]

In connection with matesaponins, a family of glycoconjugated derivatives of the pentacyclic triterpenoid named ursolic acid,[38] an extensive review recently published[51] describes the pentacyclic triterpenoids in herbal medicines and their pharmacological activities in human diabetes.

Conclusions

The dry leaves and sticks of YM displayed emission upon excitation in the UV-blue region of the electromagnetic spectrum. In particular, the fluorescence ratio blue/red excited at 360 nm was shown to be a fingerprint for each YM component (stick or leaf).

Linear correlations have been found for the different optical and spectroscopic parameters studied as a function of YM composition: BF/RF, S(669), and colour coordinates RGB (obtained either from reflectance or directly from standardized images). The best correlations were obtained for the scanned images and for the fluorescence ratio. These results open diverse interesting possibilities for determining YM composition in a non-destructive way through the linear unmixing of these optical signals. Thereby, in this work we are presenting the basis for new optical methods to assess YM quality, instead of the traditional and time consuming method of analysis by mechanical separation. In particular, standardized imaging analysis should be a reliable low cost methodology. It has been presented here for scanned images but it might easily be extended to other image acquisition techniques.

Higher TPC was found for leaves suggesting a higher nutritional value compared to sticks.

Additionally, UV-MALDI-MS and UV-LDI-MS analysis were performed for the first time on this substrate (smashed leaves, smashed sticks, infusions prepared with hot water) finding distinctive chemical profiles for leaves and sticks. These results also suggested a quite different nutraceutical value for leaves and sticks.

Abbreviations

YM	Yerba mate
SPMF	Solid phase molecular fluorescence
DRS	Diffuse reflectance spectroscopy
IM	Imaging
UV-MALDI	Ultraviolet matrix-assisted laser desorption ionization
UV-LDI	Ultraviolet laser desorption ionization
MS	Mass spectrometry
TPC	Total phenol concentration
BF	Blue fluorescence
RF	Red fluorescence
FRF	Far red fluorescence
$S(\lambda)$	Reflectance at wavelength λ
DRS	Diffuse reflectance spectroscopy
LC	Liquid chromatography
UPLC	Ultra performance liquid chromatography
PDA	Photodiode array detection
MS/MS	Tandem mass spectrometry
HPLC	High pressure liquid chromatography
ESI/IT-TOF	Electrospray/ion trap-time of flight
DAD	Diode array
LC × LC	Two-dimensional liquid chromatography
FLD	Fluorescence detector
CGA	Chlorogenic acids
LC	Liquid chromatography
CQA	Caffeoylquinic acids
GA	Galic acid

Acknowledgements

The authors are grateful to the University of Buenos Aires (UBACyT 20020130100166BA and X 0055BA), Consejo Nacional de Investigación Científica y Tecnológica (CONICET PIP 0072CO) and to the Agencia Nacional de Promoción Científica y Tecnológica (PICT 2012-2357 and 2012-0888) for the financial support. TP developed this work with a fellowship from the University of Buenos Aires. GP, REB and MGL are Research Members of CONICET (Argentina). The Ultraflex II (Bruker) TOF/TOF mass spectrometer was supported by a grant from ANPCYT, PME 125.

References

1 C. I. Heck and E. G. Mejía, Yerba Mate Tea (*Ilex paraguariensis*): A Comprehensive Review on Chemistry, Health Implications, and Technological Considerations, *J. Food Sci.*, 2007, **72**, R138–R151.

2 R. Filip, R. Davicino and C. Anesini, Antifungal activity of the aqueous extract of *Ilex paraguariensis* against *Malassezia furfur*, *Phytother. Res.*, 2010, **24**, 715–719.

3 A. Gugliucci and A. J. C. Stahl, Low-density-lipoprotein oxidation is inhibited by extracts of *Ilex Paraguariensis*, *Biochem. Mol. Biol. Int.*, 1995, **35**, 47–56.

4 M. Carini, R. M. Facino, G. Aldini, M. Calloni and L. Colombo, Characterization of phenolic antioxidants from mate (*Ilex paraguayensis*) by liquid chromatography mass spectrometry and liquid chromatography tandem mass spectrometry, *Rapid Commun. Mass Spectrom.*, 1998, **12**, 1813–1819.

5 C. Anesini, G. Ferraro and R. Filip, Peroxidase-like activity of *Ilex paraguariensis*, *Food Chem.*, 2006, **97**, 459–464.

6 L. Bravo, L. Goya and E. Lecumberri, LC/MS characterization of phenolic constituents of mate (*Ilex paraguariensis*, St. Hil.) and its antioxidant activity compared to commonly consumed beverages, *Food Res. Int.*, 2007, **40**, 393–405.

7 ANMAT Código Alimentario Argentino, Chapter XV, in *Productos estimulantes o fruitivos, Art.1193–1198*, ANMAT, Buenos Aires, 2013.

8 P. N. Prasad, in *Introduction to Biophotonics*, John Wiley & Sons, Inc., Habaken, New Jersey, 2003, pp. 1–10.

9 J. Mendes Novo, A. Iriel and M. G. Lagorio, Modelling chlorophyll fluorescence of kiwi fruit (*Actinidia deliciosa*), *Photochem. Photobiol. Sci.*, 2012, **11**, 724–730.

10 J. Mendes Novo, A. Iriel, M. C. Marchi and M. G. Lagorio, Spectroscopy, Microscopy and Fluorescence Imaging of *Origanum vulgare* L. Basis for Non-destructive Quality Assessment, *Photochem. Photobiol.*, 2013, **89**, 1383–1390.

11 F. Amaral da Silva, C. Pavei, G. González Ortega, E. Martins Lima, D. Guimarãe Almeida Diniz, J. C. Fonseca Moreira and V. J. Linck Bassani, Validation of an LC Method for Polyphenol Assay in Extractive Solutions from *Ilex paraguariensis* (Mate) *Liq. Chromatogr*, *Relat. Technol.*, 2007, **30**, 3119–3131.

12 L. M. De Souza, N. Dartora, C. T. Scoparo, T. R. Cipriani, P. A. J. Gorin, M. Iacomini and G. L. Sassaki, Comprehensive analysis of maté (*Ilex paraguariensis*) compounds: Development of chemical strategies for matesaponin analysis by mass spectrometry, *J. Chromatogr. A.*, 2011, **1218**, 7307–7315.

13 A. E. Thea, D. Ferreira, L. A. Brumovsky and M. E. Schmalko, Polycyclic aromatic hydrocarbons (PAHs) in yerba maté (*Ilex paraguariensis* St. Hil) traditional infusions (mate and tereré), *Food Control*, 2016, **60**, 215–220.

14 P. Dugo, F. Cacciola, P. Donato, R. A. Jacques;, E. B. Caramão and L. Mondello, High efficiency liquid chromatography techniques coupled to mass spectrometry for the characterization of mate extracts, *J. Chromatogr. A.*, 2009, **1216**, 7213–7221.

15 V. Marques and A. Farah, Chlorogenic Acids and Related Compounds in Medicinal Plants and Infusions, *Food Chem.*, 2008, **113**, 1370–1376.

16 D. H. Markowicz Bastos, L. A. Saldanha, R. R. Catharino, A. C. H. F. Sawaya, I. B. S. Cunha, P. O. Carvalho and M. N. Eberlin, Phenolic antioxidants identified by ESI-MS from Yerba Maté (*Ilex paraguariensis*) and green tea (*Camelia sinensis*) extracts, *Molecules*, 2007, **12**, 423–432.

17 N. Dartora, L. M. de Souza, A. P. Santana-Filho, M. Iacomini, A. T. Valduga, P. A. J. Gorin and G. L. Sassaki, UPLC-PDA-MS evaluation of bioactive compounds from leaves of *Ilex paraguariensis* with different growth conditions, treatments and ageing, *Food Chem.*, 2011, **129**, 1453–1461.

18 R. G. Peres, F. G. Tonin, M. F. M. Tavares and D. B. Rodriguez-Amaya, HPLC-DAD-ESI/MS Identification and Quantification of Phenolic Compounds in *Ilex paraguariensis* Beverages and On-Line Evaluation of Individual Antioxidant Activity, *Molecules*, 2013, **18**, 3859–3871.

19 V. Márquez, N. Martínez, M. Guerra, L. Fariña, E. Boido and E. Dellacassa, Characterization of aroma-impact compounds in yerba mate (*Ilex paraguariensis*) using GC–olfactometry and GC–MS, *Food Res. Int.*, 2013, **53**, 808–815.

20 A. H. P. Souza, R. C. G. Corrêa, L. Barros, R. C. Calhelha, C. Santos-Buelga, R. M. Peralta, A. Bracht, M. Matsushita and I. C. F. R. Ferreira, Phytochemicals and bioactive properties of *Ilex paraguariensis*: An in-vitro comparative study between the whole plant, leaves and stems, *Food Res. Int.*, 2015, **78**, 286–294.

21 W. Wendlandt and H. Hecht, Theory Diffuse Reflectance, in *Reflectance Spectroscopy*, ed. P. J. Elving and I. M. Kolthoff, Interscience Publishers, New York, 1966, pp. 46–90.

22 A. Iriel and M. G. Lagorio, Biospectroscopy of *Rhododendron indicum* flowers. Non-destructive assessment of anthocyanins in petals using a reflectance-based method, *Photochem. Photobiol. Sci.*, 2009, **8**, 337–344.

23 H. Jahn, Foundations and Definitions, in *Digital Airborne Camera: Introductionand Technology*, ed. R. Sandau, Springer, DLR, Berlin, Germany, 2010, ch2., section 2.7, pp. 89–94.

24 S. Chandra, S. Khan, B. Avula, H. Lata, M. H. Yang, M. A. ElSohly and I. A. Khan, Assessment of Total Phenolic and Flavonoid Content, Antioxidant Properties, and Yield of Aeroponically and Conventionally Grown Leafy Vegetables and Fruit Crops: A Comparative Study, *J. Evid-Based Complementary Altern. Med.*, 2014, 253875, DOI: 10.1155/2014/253875, 9 pages, (accessed December 2015).

25 H. Nonami, S. Fukui and R. Erra-Balsells, β-Carboline Alkaloids as Matrices for Matrix-assisted Ultraviolet Laser Desorption Time-of-flight Mass Spectrometry of Proteins and Sulfated Oligosaccharides: a Comparative Study Using Phenylcarbonyl Compounds, Carbazoles and Classical Matrices, *J. Mass Spectrom.*, 1997, **32**, 287–296.

26 M. Lang and H. K. Lichtenthaler, Changes in the Blue-Green and Red Fluorescence-Emission Spectra of Beech Leaves during the Autumnal Chlorophyll Breakdown, *J. Plant Physiol.*, 1991, **138**, 550–553.

27 M. Lang, F. Stober and H. K. Lichtenthaler, Fluorescence emission spectra of plant leaves and plant constituents, *Radiat. Environ. Biophys.*, 1991, **30**, 333–347.

28 A. P. Nifli, P. A. Theodoropoulos, S. Munier, C. Castagnino, E. Roussakis, H. E. Katerinopoulos, J. Vercauteren and E. Castanas, Quercetin exhibits a specific fluorescence in cellular milieu: A valuable tool for the study of its intracellular distribution, *J. Agric. Food Chem.*, 2007, **55**, 2873–2878.

29 N. R. Baker, Chlorophyll fluorescence: A probe of photosynthesis in vivo, *Annu. Rev. Plant Biol.*, 2008, **59**, 89–113.

30 Govindjee, Chlorophyll a Fluorescence: A Bit of Basics and History, in *Chlorophyll a Fluorescence – A Signature of Photosynthesis*, ed. G. Papageorgiou and Govindjee, Springer, Dordrecht, 2004, vol. 19, pp. 1–32.

31 M. G. Lagorio, Chlorophyll fluorescence emission spectra in photosynthetic organisms, in *Chlorophyll: Structure,*

Production and Medicinal Uses, ed. L. Hua and S. Elisa, Nova Science Publishers, New York, 2011, pp. 115–150.
32 J. F. Mustard and J. M. Sunshine, Spectral Analysis for Earth Science Investigation, in *Manual of Remote Sensing, Remote Sensing for the Earth Sciences*, ed. A. N. Rencz and R. A. Ryerson, John Wiley and Sons, New York, 1999, vol. 3, p. 293.
33 R. E. Milliken and J. F. Mustard, Estimating the water content of hydrated minerals using reflectance spectroscopy I. Effects of darkening agents and low-albedo materials, *Icaru*, 2007, **189**, 550–573.
34 J. F. Mustard and C. M. Pieters, Photometric Phase Functions of Common Geologic Minerals and Applications to Quantitative Analysis of Mineral Mixture Reflectance Spectra, *J. Geophys. Res.*, 1989, **94**, 13619–13634.
35 S. Chandra and E. Gonzalez de Mejia, Polyphenolic Compounds, Antioxidant Capacity, and Quinone Reductase Activity of an Aqueous Extract of *Ardisia compressa* in Comparison to Mate (*Ilex paraguariensis*) and Green (*Camellia sinensis*) Teas, *J. Agric. Food Chem.*, 2004, **52**, 3583–3589.
36 J. M. Landete, Dietary Intake of Natural Antioxidants: Vitamins and Polyphenols, *Crit. Rev. Food Sci.*, 2013, **53**, 706–721.
37 E. L. da Silva, T. J. C. Neiva, M. Shirai, J. Terao and D. S. P. Abdalla, Acute ingestion of yerba mate infusion (*Ilex paraguariensis*) inhibits plasma and lipoprotein oxidation, *Food Res. Int.*, 2008, **41**, 973–979.
38 G. Gosmann and D. Guillaume, Triterpenoid saponins from *Ilex paraguariensis*, *J. Nat. Prod.*, 1995, **58**, 438–441.
39 H. Luo, B. H. Jiang, S. M. King and Y. C. Chen, Inhibition of cell growth and VEGF expression in ovarian cancer cells by flavonoids, *Nutr. Cancer*, 2008, **60**, 800–809.
40 R. S. Chauhan, N. Gupta, S. K. Sharma, J. C. Rana, T. R. Sharma and S. Jana, Genetic and genome resources in Buckwheat- Present and Future Perspectives, *Eur. J. Plant Sci. Biotechnol.*, 2010, **4**, 33–44.
41 T. Shohaib, M. Shafique, N. Dhanya and M. C. Divakar, Importance of Flavonoides in Therapeutics, *Hygeia: J. Drugs Med.*, 2011, **3**, 1–18.
42 N. Kamalakkannan and P. S. Prince, Antihyperglycaemic and antioxidant effect of rutin, a polyphenolic flavonoid, in streptozotocin-induced diabetic wistar rats, *Basic Clin. Pharmacol. Toxicol.*, 2006, **98**, 97–103.
43 P. X. Xu, S. W. Wang, X. L. Yu, Y. J. Su, T. Wang, W. W. Zhou, H. Zhang, Y. J. Wang and R. T. Liu, Rutin improves spatial memory in Alzheimer's disease transgenic mice by reducing Aβ oligomer level and attenuating oxidative stress and neuroinflammation, *Behav. Brain Res.*, 2014, **264**, 173–180.
44 T. Guardia, A. E. Rotelli, A. O. Juarez and L. E. Pelzer, Anti-inflammatory properties of plant flavonoids. Effects of rutin, quercetin and hesperidin on adjuvant arthritis in rat, *Farmaco*, 2001, **56**, 683–687.
45 D. D. Orhan, B. Özçelik, S. Özgen and F. Ergun, Antibacterial, antifungal, and antiviral activities of some flavonoids, *Microbiol. Res.*, 2010, **165**, 496–504.
46 O. Danino, H. E. Gottlieb, S. Grossman and M. Bergman, Antioxidant activity of 1,3-dicaffeoylquinic acid isolated from *Inula viscose*, *Food Res. Int.*, 2009, **42**, 1273–1280.
47 S. Hong, T. Joo and J.-W. Jhoo, Antioxidant and anti-inflammatory activities of 3,5-dicaffeoylquinic acid isolated from *Ligularia fischeri* leaves, *Food Sci. Biotechnol.*, 2015, **24**, 257–263.
48 W. E. Robinson Jr., M. Cordeiro, S. Abdel-Malek, Q. Jia, S. A. Chow, M. G. Reinecke and W. M. Mitchell, Dicaffeoylquinic acid inhibitors of human immunodeficiency virus integrase: inhibition of the core catalytic domain of human immunodeficiency virus integrase, *Mol. Pharmacol.*, 1996, **50**, 846–855.
49 R. B. An, D. H. Sohn, G. S. Jeong and Y. C. Kim, *In vitro* hepatoprotective compounds from *Suaeda glauca*, *Arch. Pharm. Res.*, 2008, **31**, 594–597.
50 E. Madrigal-Santillán, E. Madrigal-Bujaidar, I. Álvarez-González, M. T. Sumaya-Martínez, J. Gutiérrez-Salinas, B. Mirandeli, A. Morales-González, M. García-Luna, J. González-Rubio, L. Aguilar-Faisal and J. A. Morales-González, Review of natural products with hepatoprotective effects, *World J. Gastroenterol.*, 2014, **20**, 14787–14804.
51 A. Alqahtani, K. Hamid, A. Kam, K. H. Wong, Z. Abdelhak, V. Razmovski-Naumovski, K. Chan, K. M. Lic, P. W. Groundwater and G. Q. Li, The pentacyclic triterpenoids in herbal medicines and their pharmacological activities in diabetes and diabetic complications, *Curr. Med. Chem.*, 2013, **20**, 908–931.

